

Superluminal and slow light in Λ -type three-level atoms via squeezed vacuum and spontaneously generated coherence

F. Carreño,¹ Oscar G. Calderón,¹ M. A. Antón,¹ and Isabel Gonzalo²¹*Escuela Universitaria de Óptica, Universidad Complutense de Madrid, C/ Arcos de Jalón s/n, 28037 Madrid, Spain*²*Facultad de Ciencias Físicas, Universidad Complutense de Madrid, Ciudad Universitaria s/n, 28040, Spain*

(Received 26 November 2004; revised manuscript received 24 February 2005; published 15 June 2005)

We study the dispersion and absorption spectra of a weak probe in a Λ -type three-level atomic system with closely ground sublevels driven by a strong field and damped by a broadband squeezed vacuum. We analyze the interplay between the spontaneous generated coherence and the squeezed field on the susceptibility of the atomic system. We find that by varying the intensity of the squeezed field the group velocity of a weak pulse can change from subluminal to superluminal. In addition we exploit the fact that the properties of the atomic medium can be dramatically modified by controlling the relative phase between the driving field and the squeezed field, allowing us to manipulate the group velocity at which light propagates. The physical origin of this phenomenon corresponds to a transfer of the atomic coherence from electromagnetically induced transparency to electromagnetically induced absorption. Besides, this phenomenon is achieved under nearly transparency conditions and with negligible distortion of the propagation pulse.

DOI: 10.1103/PhysRevA.71.063805

PACS number(s): 42.50.Gy, 32.80.-t, 42.50.Dv

I. INTRODUCTION

In recent years, there has been a renewed interest in the study of subluminal and superluminal light propagation in atomic media having very special controlled optical properties. Slow group velocity in coherent media has been shown to provide new regimes of nonlinear interaction with highly increased efficiency even for very weak light fields. It has been demonstrated that electromagnetically induced transparency (EIT) is accompanied by large frequency dispersion [1–4], thus the group velocity can be slowed down up to $10\text{--}10^2$ m/s [5,6]. Harris and co-workers have found that large positive dispersion of refractive index in the EIT window can be used to reduce dramatically the group velocity of light pulses [5], which leads to nonlinear optics at low light level [7], and quantum memory [8]. Kocharovskaya *et al.* [9] showed how the spatial dispersion can even stop light in a hot gas. Using EIT and adiabatic following of *dark state polaritons*, the group velocity of light pulses can be dramatically decelerated and their quantum state can be mapped into a metastable collective state of atomic ensembles [10], which is of application in quantum information. On the other side, superluminal propagation occurs in optical media with anomalous dispersion [11]. Wang *et al.* [12] demonstrated superluminal light propagation using the region of lossless anomalous dispersion between two closely spaced gain lines in a double-peaked Raman gain medium. The gain doublet is created by applying two intense detuned cw pumps with slightly different frequencies to one transition of a Λ -type three-level system in atomic cesium. Another important consequence of quantum coherence, the so-called electromagnetically induced absorption (EIA), can lead to a highly anomalous dispersion where enhanced absorption occurs [13–15]. Akulshin *et al.* [16] and Kim *et al.* [17] reported experiments where negative group velocities of $v_g = -c/14\,400$ were achieved in Cs vapor cells. It is worth noting that anomalous dispersion obtained in these systems

occurs, in general, with some absorption or gain, a non-desirable feature for propagation of pulses with negligible distortion. Recently, light propagation from subluminal to superluminal in Λ -type and V-type three-level atoms has been shown [18–20]. The control of the dispersion from normal to anomalous has been obtained by (i) applying a field connecting the two closed sublevels, and (ii) considering spontaneously generated coherence (SGC). Bigelow *et al.* [21] have observed experimentally superluminal and ultraslow light propagation in an alexandrite crystal measuring group velocities as slow as 91 ms^{-1} to as fast as -800 ms^{-1} . In this experiment the phenomenon was attributed to coherent population oscillations. In recent works, subluminal and superluminal propagation have been theoretically predicted. Agarwal and Dasgupta [22] have shown superluminal propagation via coherent manipulation of Raman gain processes in N-type atoms. Sahrai *et al.* [23] have shown tunable phase control from subluminal to superluminal light propagation in an Λ -type atom with an extra energy level. Experimental evidences of fast and slow light propagation in four-level atoms have been obtained [24,25].

In view of the many potential applications of subluminal and superluminal light propagation, a natural question is how one can have a controlling parameter for switching from one to the other regime of light propagation. In this paper we show theoretically the possibility of light propagation from subluminal to superluminal in Λ -type atoms with closely spaced lower levels, when the atom is driven by a strong coherent field and damped by a broadband squeezed vacuum (SV). The combined effect of the SV field and the SGC produces a small gain or absorption over a large bandwidth which makes this configuration very attractive for propagation of pulses without strong distortion in both the subluminal and superluminal regimes. We find that this phenomenon arises from the transition from EIT to EIA when the intensity of the squeezed vacuum increases. This transition can also be induced by varying the relative phase between the driving field to the squeezed field.

The existence of SGC effects in Λ -type atoms, which is not obvious due to the fact that there are two final possible lower states, was predicted by Javanian [26]. SGC has been proved to significantly modify the optical properties of the atomic system [26–31]. The role played by the squeezed vacuum (SV) fluctuations in the atomic dynamics has been a subject of intense activity since the seminal work due to Gardiner [32]. Ficek *et al.* [33] have shown that a two-level atom damped by a broadband squeezed vacuum can exhibit a strong emission peak (gain) at the central frequency of the atomic levels, which is not attributed to population inversion, and results from the so-called *coherent population oscillations* [34]. Akram *et al.* [35] have studied the index of refraction of a two-level atom replacing the usually applied coherent field by a squeezed vacuum field. They showed that the system can produce a large, although not maximum, index of refraction accompanied by vanishing absorption when the carrier frequency of squeezed vacuum is detuned from the atomic resonance. So far, however, the driven multilevel systems interacting with squeezed vacuum have been considered only towards exploiting the fluorescent properties [36,37].

The paper is organized as follows: Section II establishes the model, i.e., the Hamiltonian of the system and the evolution equation of the atomic operators assuming the rotating wave approximation. Section III is devoted to present the effects of SGC and the SV on the absorptive and dispersive properties of the atomic medium, and in the group velocity of a weak pulse. A discussion of the numerical results is present in Sec. IV. Finally, Sec. V summarizes the main conclusions.

II. ATOMIC MODEL AND DENSITY-MATRIX EQUATIONS

We consider a closed, Λ -type three-level system with two near-degenerate levels $|1\rangle$ and $|2\rangle$, and an excited level $|3\rangle$ as shown in Fig. 1(a). Transition $|3\rangle \leftrightarrow |2\rangle$ is driven by an external coherent field \vec{E} given by

$$\vec{E} = \frac{1}{2} \vec{E}_0(t) e^{-i(\omega_L t + \phi)} + \text{c.c.}, \quad (2.1)$$

$\vec{E}_0(t)$ being the slowly varying field envelope, whereas ω_L , and ϕ are the angular frequency and the phase of the field, respectively.

In order to take into account the induced-coherence effects by spontaneous emission, the upper level $|3\rangle$ is coupled to lower levels $|2\rangle$ and $|1\rangle$ by the same vacuum modes. The resonant frequencies between the upper level $|3\rangle$ and the ground levels $|2\rangle$ and $|1\rangle$ are ω_{32} and ω_{31} , respectively. Note that $\omega_{32} - \omega_{31} = \omega_{21}$, ω_{21} being the frequency separation of the lower levels.

The Hamiltonian of the system in the rotating wave approximation is given by [38,39]

$$H = \hbar \sum_{m=1}^3 \omega_m |m\rangle \langle m| + \hbar \sum_{k\lambda} \omega_{k\lambda} a_{k\lambda}^\dagger a_{k\lambda} - \hbar \sum_{m=1}^2 \sum_{k\lambda} g_{mk} a_{k\lambda} |3\rangle \langle m| - \text{H.c.} - \hbar \Omega e^{-i(\omega_L t + \phi)} |3\rangle \langle 2| - \text{H.c.}, \quad (2.2)$$

where $\hbar \omega_m$ are the energies of the atomic levels, and $a_{k\lambda} (a_{k\lambda}^\dagger)$

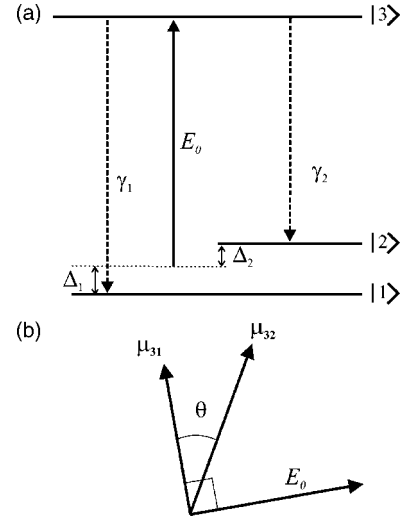


FIG. 1. (a) Λ -type atom driven by a coherent field E_0 of frequency ω_L and phase ϕ . γ_1 and γ_2 are the decay rates from the excited level $|3\rangle$ to levels $|1\rangle$, and $|2\rangle$, respectively. (b) The polarization arrangement.

is the annihilation (creation) operator of the k th mode of the vacuum field with polarization $\vec{e}_{k\lambda}$ ($\lambda=1,2$) and angular frequency $\omega_{k\lambda}$. The parameter g_{mk} is the coupling constant of the atomic transition $|m\rangle \leftrightarrow |3\rangle$ with the vacuum electromagnetic mode

$$g_{mk} = \sqrt{\frac{\omega_{k\lambda}}{2\hbar\epsilon_0 V}} (\vec{\mu}_{3m} \cdot \vec{e}_{k\lambda}), \quad (2.3)$$

where $\vec{\mu}_{3m}$ is the dipolar moment of the transition $|m\rangle \leftrightarrow |3\rangle$. $\Omega = \vec{\mu}_{32} \cdot \vec{E}_0 / (2\hbar)$ is the Rabi frequency of the transition $|2\rangle \leftrightarrow |3\rangle$. We consider the polarization arrangement shown in Fig. 1(b), i.e., $\vec{\mu}_{31} \cdot \vec{E}_0 = 0$.

We now assume that the quantized radiation field is in a broadband squeezed vacuum state with carrier frequency ω_v , which is tuned close to the frequency of the atomic transitions $|3\rangle \leftrightarrow |1\rangle$ and $|3\rangle \leftrightarrow |2\rangle$, that is, $2\omega_v \approx \omega_{31} + \omega_{32}$. The bandwidth of the squeezed field is assumed to be broad enough so that the squeezed vacuum appears as δ -correlated squeezed white noise to the atom. The correlation function for the field operators $a(\omega_{k\lambda})$ and $a^\dagger(\omega_{k\lambda})$ can be written as [32,36]

$$\langle a(\omega_{k\lambda}) a^\dagger(\omega'_{k\lambda}) \rangle = [N(\omega_{k\lambda}) + 1] \delta(\omega_{k\lambda} - \omega'_{k\lambda}),$$

$$\langle a^\dagger(\omega_{k\lambda}) a(\omega'_{k\lambda}) \rangle = N(\omega_{k\lambda}) \delta(\omega_{k\lambda} - \omega'_{k\lambda}),$$

$$\langle a(\omega_{k\lambda}) a(\omega'_{k\lambda}) \rangle = M(\omega_{k\lambda}) \delta(2\omega_v - \omega_{k\lambda} - \omega'_{k\lambda}), \quad (2.4)$$

$N(\omega_{k\lambda})$ and $M(\omega_{k\lambda})$ being slowly varying functions of the frequency that characterize the squeezing. Note that M is a complex magnitude so that $M(\omega_{k\lambda}) = |M(\omega_{k\lambda})| e^{i\phi_v}$, where ϕ_v is the phase of the squeezed vacuum. For $M(\omega_{k\lambda}) = 0$, Eq. (2.4) describes a thermal field at a finite temperature T , where $N(\omega_{k\lambda})$ is the mean occupation number of the mode $k\lambda$ with frequency $\omega_{k\lambda}$.

The system is studied using the density-matrix formalism. By following the traditional approach of Weisskopf and Wigner [38,40], we have re-derived the master equation, in

an appropriate interaction picture, for the reduced density matrix of the atomic system, $\rho_s^{(I)}$, in the Born and Markov approximation, which read as

$$\begin{aligned} \frac{\partial \rho_s^I}{\partial t} = & -\frac{i}{\hbar}[H_{ex}^I, \rho_s^I] - \frac{N+1}{2}(\gamma_1 + \gamma_2)(\sigma_{33}\rho_s^I + \rho_s^I\sigma_{33}) - \frac{N}{2}[\gamma_1(\sigma_{11}\rho_s^I + \rho_s^I\sigma_{11}) + \gamma_2(\sigma_{22}\rho_s^I + \rho_s^I\sigma_{22}) + \gamma_{12}(\sigma_{12}\rho_s^I e^{-i\omega_{21}t} + \rho_s^I\sigma_{21} e^{i\omega_{21}t}) \\ & + \gamma_{12}(\sigma_{21}\rho_s^I e^{i\omega_{21}t} + \rho_s^I\sigma_{12} e^{-i\omega_{21}t})] + (N+1)[\gamma_1\sigma_{13}\rho_s^I\sigma_{31} + \gamma_2\sigma_{23}\rho_s^I\sigma_{32} + \gamma_{12}\sigma_{13}\rho_s^I\sigma_{32} e^{-i(\omega_{31}-\omega_{32})t} + \gamma_{12}\sigma_{23}\rho_s^I\sigma_{31} e^{i(\omega_{31}-\omega_{32})t}] \\ & + N[\gamma_1\sigma_{31}\rho_s^I\sigma_{13} + \gamma_2\sigma_{32}\rho_s^I\sigma_{23} + \gamma_{12}\sigma_{31}\rho_s^I\sigma_{23} e^{i(\omega_{31}-\omega_{32})t} + \gamma_{12}\sigma_{32}\rho_s^I\sigma_{13} e^{-i(\omega_{31}-\omega_{32})t}] + M[\gamma_1\sigma_{31}\rho_s^I\sigma_{31} e^{-i(2\omega_v-2\omega_{31})t} \\ & + \gamma_2\sigma_{32}\rho_s^I\sigma_{32} e^{-i(2\omega_v-2\omega_{32})t} + \gamma_{12}\sigma_{31}\rho_s^I\sigma_{32} e^{-i(2\omega_v-\omega_{31}-\omega_{32})t} + \gamma_{12}\sigma_{32}\rho_s^I\sigma_{31} e^{-i(2\omega_v-\omega_{32}-\omega_{31})t}] + M^*[\gamma_1\sigma_{13}\rho_s^I\sigma_{13} e^{i(2\omega_v-2\omega_{31})t} \\ & + \gamma_2\sigma_{23}\rho_s^I\sigma_{23} e^{i(2\omega_v-2\omega_{32})t} + \gamma_{12}\sigma_{13}\rho_s^I\sigma_{23} e^{i(2\omega_v-\omega_{31}-\omega_{32})t} + \gamma_{12}\sigma_{23}\rho_s^I\sigma_{13} e^{i(2\omega_v-\omega_{32}-\omega_{31})t}], \end{aligned} \quad (2.5)$$

where

$$H_{ex}^I = -\hbar\Delta_1\sigma_{33} - \hbar(\Delta_1 - \Delta_2)\sigma_{22} - \hbar(\Omega\sigma_{32} + \text{H.c.}) \quad (2.6)$$

represents the interaction between the atom and the external driving field in the interaction picture. $\Delta_1 = \omega_L - \omega_{31}$ and $\Delta_2 = \omega_L - \omega_{32}$ are the optical detunings. The notation $\sigma_{mn} = |m\rangle\langle n|$ for the atomic operators has been introduced, and γ_1, γ_2 are the decay rates for the $|3\rangle \leftrightarrow |1\rangle$ and $|3\rangle \leftrightarrow |2\rangle$ transitions, respectively. The damping terms proportional to γ_{12} in Eq. (2.5) are particularly important when $\omega_{21} \approx \gamma_1, \gamma_2$, and they arise due to the coupling of the two transitions $|3\rangle \leftrightarrow |1\rangle$ and $|3\rangle \leftrightarrow |2\rangle$ with the same vacuum mode. They are responsible for the quantum interference between the two decay

channels [41]. It can be seen that these terms oscillate at the frequency difference $\omega_{31} - \omega_{32}$, thus when this difference is large enough, they may be dropped. This is the case treated in Ref. [36]. The present discussion is based on the situation where $\omega_{31} \approx \omega_{32}$, so such nonsecular terms must be retained. In addition, it can be shown [38] that

$$\gamma_{12} = \sqrt{\gamma_1 \gamma_2} p \quad (2.7)$$

and $p = \vec{\mu}_{31} \cdot \vec{\mu}_{32} / |\vec{\mu}_{31}| |\vec{\mu}_{32}| = \cos \theta$ denotes the alignment of the dipole moments $\vec{\mu}_{31}$ and $\vec{\mu}_{32}$.

Through an appropriate unitary transformation we eliminate the explicit temporal dependence in the master equation, and obtain the evolution equations of the density-matrix elements,

$$\frac{\partial \rho_{33}}{\partial t} = -[(N+1)(\gamma_1 + \gamma_2) + N\gamma_{12}]\rho_{33} + N\gamma_{12}(\rho_{12} + \rho_{21}) + i\Omega(\rho_{23} - \rho_{32}) + N(\gamma_2 - \gamma_1)\rho_{22} + N\gamma_2,$$

$$\frac{\partial \rho_{22}}{\partial t} = (N+1)\gamma_2\rho_{33} - N\frac{\gamma_{12}}{2}(\rho_{12} + \rho_{21}) - N\gamma_2\rho_{22} - i\Omega(\rho_{23} - \rho_{32}),$$

$$\frac{\partial \rho_{31}}{\partial t} = -F_{31}\rho_{31} + i\Omega\rho_{21} - N\frac{\gamma_{12}}{2}\rho_{32} + |M|\gamma_1 e^{-i\Phi}\rho_{13} + |M|\gamma_{12} e^{-i\Phi}\rho_{23},$$

$$\frac{\partial \rho_{21}}{\partial t} = -F_{21}\rho_{21} + (3N+2)\frac{\gamma_{12}}{2}\rho_{33} + i\Omega\rho_{31} - N\frac{\gamma_{12}}{2},$$

$$\frac{\partial \rho_{32}}{\partial t} = -F_{32}\rho_{32} + |M|\gamma_{12} e^{-i\Phi}\rho_{13} - N\frac{\gamma_{12}}{2}\rho_{31} - i\Omega(\rho_{33} - \rho_{22}) + |M|\gamma_2 e^{-i\Phi}\rho_{23}, \quad (2.8)$$

where

$$\begin{aligned} F_{31} &= \left[\frac{(N+1)}{2}(\gamma_1 + \gamma_2) + \frac{N}{2}\gamma_1 - i\Delta_1 \right], \\ F_{21} &= \left[\frac{N}{2}(\gamma_1 + \gamma_2) - i(\Delta_1 - \Delta_2) \right], \\ F_{32} &= \left[\frac{(N+1)}{2}(\gamma_1 + \gamma_2) + \frac{N}{2}\gamma_2 - i\Delta_2 \right], \end{aligned} \quad (2.9)$$

and the relative phase

$$\Phi = \phi_v - 2\phi, \quad (2.10)$$

which represents the phase difference between the coherent field and the squeezing field. The terms related to $p = \gamma_{12}/\sqrt{\gamma_1\gamma_2} = \cos\theta$ in Eq. (2.8) represent the effect of the quantum interference arising from the cross coupling between spontaneous emissions $|3\rangle \leftrightarrow |1\rangle$ and $|3\rangle \leftrightarrow |2\rangle$. The parameter p depends on the angle θ between the two transition dipole moments. Due to the polarization arrangement considered in Fig. 1(b) $p < 1$ and $p=0$ represents the case of no quantum interference. In the context of inversionless gain studies, the main difference between our equations and those analyzed by other authors [26,29] are the terms proportional to N and M , which account for the presence of the squeezed vacuum field. This fact modifies the equations in an important way: in the absence of squeezed vacuum, the interference term only appears in the equation of the coherence ρ_{21} , and it is proportional to the population of the excited level ρ_{33} . However, the presence of squeezed vacuum makes the interference parameter p appear in the equation of motion of all coherences and populations [see Eq. (2.8)]. We can also see that coherences depend on the correlations between pairs of modes in the reservoir which leads to a phase sensitivity in the optical response.

III. EFFECT OF SGC AND SV ON THE ABSORPTIVE AND DISPERSIVE PROPERTIES OF ATOMIC MEDIUM

We are interested in analyzing the behavior of a probe signal which drives transition $|3\rangle \rightarrow |1\rangle$. To do that, we suppose that after the system has reached the steady state, the atom is perturbed by a weak probe field of frequency ω_p . The probe intensity is assumed to be sufficiently weak that does not produce a noticeable perturbation of the atom-driving-field system. This will allow us to determine the dispersive and absorptive properties of the medium and to analyze how a pulse propagates inside the medium in the presence of both the driving field and the SV field. Thus we will need to determine the linear susceptibility which is defined as

$$A(\omega_p) = \int_0^\infty \lim_{t \rightarrow \infty} \langle [D^-(t' + t), D^+(t)] \rangle e^{-i(\omega_p - \omega_L)t'} dt', \quad (3.1)$$

where $D^-(t) = d_{13}\sigma_{13}(t)$ is the slowly varying part of the atomic polarization operator in the direction of the probe

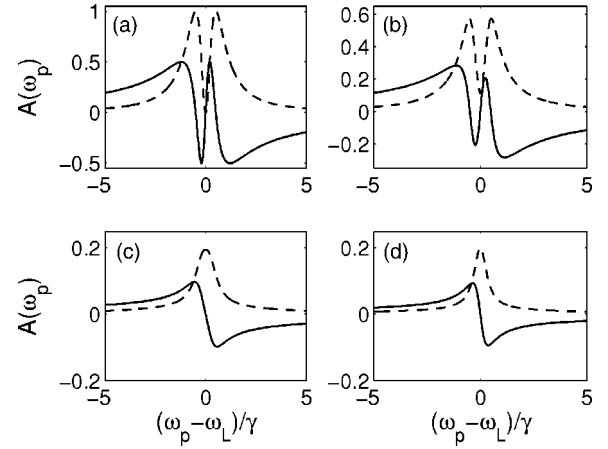


FIG. 2. Real (dashed line) and imaginary (solid line) parts of the absorption spectrum $A(\omega_p)$ of the weak probe field versus the dimensionless frequency difference $(\omega_p - \omega_L)/\gamma$. The parameters are $\gamma_1 = \gamma_2 \equiv \gamma$, $\Omega = 0.5\gamma$, $\Delta_2 = 0$, $\omega_{21} = 0$, $p = 0.99$, and $\Phi = 0$. The mean photon number is (a) $N=0$, (b) $N=0.1$, (c) $N=0.7$, and (d) $N=1$. A perfect squeezing condition $[|M| = \sqrt{N(N+1)}]$ is assumed.

field polarization vector \vec{e}_p , with $d_{13} = \vec{e}_p \cdot \vec{\mu}_{31}$. The commutator is calculated in the absence of the probe field, but the squeezed vacuum and the driving field are always present. We can obtain the linear susceptibility with the help of the quantum regression theorem and the Bloch Eq. (2.8). The details of the calculation are provided in the Appendix.

We proceed to analyze how SGC and SV modifies the absorptive-dispersive properties of the probe field by analyzing $A(\omega_p)$ given by Eq. (3.1). The linear probe absorption and the index of refraction are related with the real and imaginary parts of $A(\omega_p)$, respectively. In this way, a negative value of $\text{Re}[A(\omega_p)]$ means that the system exhibits gain. In the calculations we set $\gamma_1 = \gamma_2 \equiv \gamma$. For the sake of simplicity, we consider a degenerate Λ -type atom, i.e., $\omega_{21} = 0$, and the driving field at resonance with transition $|2\rangle \rightarrow |3\rangle$ ($\Delta_2 = 0$). We also assume a perfect squeezing condition, i.e., $|M| = \sqrt{N(N+1)}$.

The absorptive-dispersive properties of the probe field are of interest when considering the propagation of a weak probe pulse. The group velocity can be modified by changing the slope of the dispersion curve. It is well known that when the probe absorption spectrum is characterized by a strong deep at resonance the phenomenon is called EIT. However, when the absorption spectrum presents a sharp peak at resonance, the phenomenon is called electromagnetically induced absorption (EIA) [16]. In order to carry out all kinds of propagation velocities we have to control atomic coherence of EIT and EIA. Generally, EIA cannot be generated in conventional three-level atomic systems. However, we will show in this work that SGC and SV can lead the atomic system from EIT to EIA. Thus a probe pulse will propagate in the subluminal (superluminal) regime if nearly EIT (EIA) conditions hold. Figure 2 displays the real and imaginary parts of $A(\omega_p)$ as a function of the dimensionless frequency difference $(\omega_p - \omega_L)/\gamma$ for different values of the mean photon number N , where we assume $p = 0.99$, $\Omega = 0.5\gamma$, and $\Phi = 0$. Note that when the system is damped by the standard vacuum, i.e.,

$N=M=0$, the probe line shape shows absorption at the Rabi sidebands, and transparency at the center, where the slope of the dispersion becomes very steep and positive [see Fig. 2(a)]. This is a well-known result, in agreement with Ref. [1], and leads to subluminal group velocity. The behavior of the system for small values of N resembles that obtained in the case with $N=0$, although it is obvious that SV partially destroys EIT and negligible absorption at $\omega_p=\omega_L$ takes place. For a weak SV, $N=0.1$, the absorption peaks are lowered and the slope of the dispersion curve at $\omega_p=\omega_L$ has decreased in comparison with the case $N=0$, but it remains positive [see Fig. 2(b)]. By increasing the photon number N up to $N=0.7$, the optical response of the system is completely modified. A sharp absorption peak (EIA) at $\omega_p=\omega_L$ appears [see Fig. 2(c)]. Furthermore, the slope of the index of refraction at $\omega_p=\omega_L$ changes its sign from positive to negative. Thus depending on the value of N we can change from the subluminal to the superluminal regime of pulse propagation. This striking physical situation arises from the fact that the linewidth of the absorption spectrum in the EIA regime is much narrower than the natural linewidth, allowing a large negative slope of the refractive index at $\omega_p=\omega_L$. We remind here that according to the Kramers-Kronig relations, any change in the absorption of the medium will be accompanied by the corresponding change in the dispersion. In Fig. 2(d) we show that a further increase of N up to $N=1$ leads to a moderate absorption at $\omega_p=\omega_L$ whereas the slope of the dispersion becomes steeper than in Fig. 2(c). In summary, Fig. 2 clearly reveals that the squeezing field can convert an EIT atomic medium into an EIA atomic medium by increasing the photon number. In other words, the squeezed vacuum can act as a knob for changing pulse propagation from subluminal to superluminal.

The group index n_g of the probe field is given by the following expression:

$$n_g \equiv \frac{c}{v_g} = 1 + \frac{\chi'(\omega_p)}{2} + \frac{\omega_p}{2} \frac{\partial}{\partial \omega_p} \chi'(\omega_p), \quad (3.2)$$

where v_g is the group velocity, and $\chi'(\omega_p)$ is the real part of the susceptibility, which is related to $A(\omega_p)$ according to

$$\chi'(\omega_p) = \frac{N_a}{2\epsilon_0\hbar\gamma} \text{Im}[A(\omega_p)], \quad (3.3)$$

N_a being the atomic density. The group index n_g can be larger than unity (subluminal light) when the dispersion is positive in the region of $\chi'(\omega_p) \approx 0$, and can be less than unity (superluminal light) when the dispersion is negative in this region. Let us analyze the time delay ΔT in the propagation of a pulse through the medium with regard to free space, which is defined as

$$\Delta T = \frac{L}{c}(n_g - 1) = \frac{L}{c} \frac{N_a \omega_p}{4\epsilon_0\hbar\gamma} \text{Im} \left[\frac{\partial A(\omega_p)}{\partial \omega_p} \right], \quad (3.4)$$

L being the length of the sample.

In order to calculate the time delay of the transmitted pulse in a realistic situation, we consider the data of the experiment of Hau *et al.* [6] carried out in a medium consisting of cold three-level atoms. The parameters are

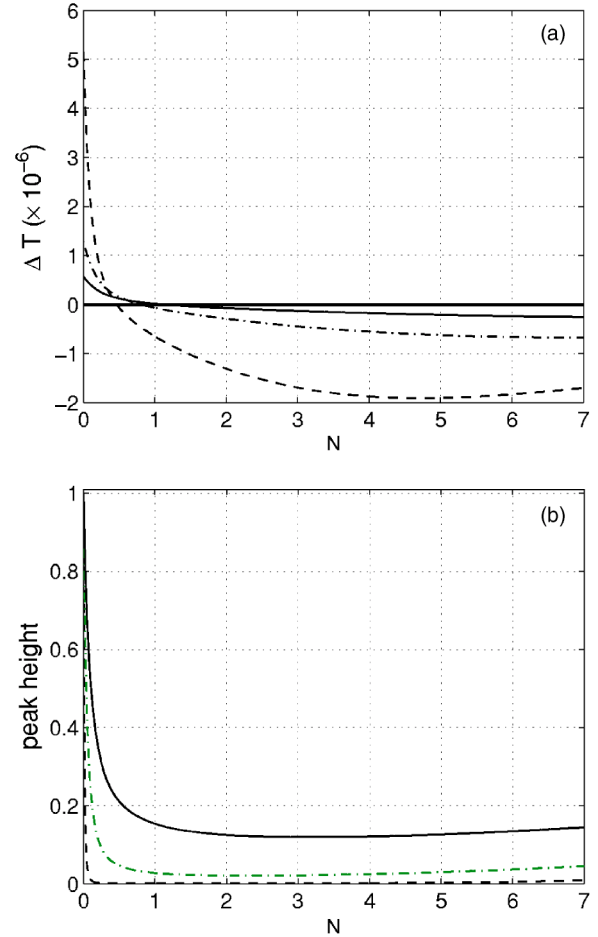


FIG. 3. (a) Time delay defined in Eq. (3.4) versus the mean photon number of the squeezed vacuum N for different values of the Rabi frequency of the driving field Ω : $\Omega=0.5\gamma$ (dashed line), $\Omega=1\gamma$ (dashed-dotted line), and $\Omega=1.5\gamma$ (solid line). The horizontal thick solid line is a reference line that allows to determine the crossing of the curves from the subluminal to the superluminal regime. We consider $|M|=\sqrt{N(N+1)}$, and $\Phi=0$. (b) Peak reduction versus the mean photon number for the Rabi frequencies considered in (a).

$N_a\mu_{31}^2/(4\epsilon_0\gamma\hbar)=0.013$, $\omega_L/\gamma=1.02\times 10^8$, and $\gamma/2\pi=5$ MHz. The sample length was $L=229\times 10^{-6}$ m. In Fig. 3(a), we plot ΔT versus the mean photon number of the squeezed vacuum (N) for different values of the Rabi frequency of the driving field Ω . We consider $\omega_p=\omega_L$ and the rest of parameters are those used in Fig. 2. We see that with the increase of N , the pulse delay changes from positive to negative. Thus the group velocity can be controlled by adjusting the photon number of the squeezed field and the propagation can change from subluminal to superluminal. The time interval at which delay can be varied increases as the Rabi frequency of the driving field decreases [see Fig. 3(a)]. It is to be noted that the change from the subluminal to the superluminal regime of pulse propagation cannot be produced when the atom is damped by a thermal field at finite temperature ($M=0$), i.e., the two-photon correlation is essential to produce the change in the sign of the dispersion.

The change in the slope of the dispersion is always accompanied by a modification in the value of the absorption at

$\omega_p = \omega_L$. Thus a compromise between the absorption and the value of the slope of the dispersion must be reached in order to get observable effects: the largest the values in the slope of the dispersion [see dashed line in Fig. 3(a)], the largest the values in the absorption (not shown), thus producing a reduction in the peak height of the transmitted pulse. In order to analyze the propagation of the pulse, we consider again the data of the experiment of Hau *et al.* [6]. We present in Fig. 3(b) the peak reduction of a Gaussian pulse $E_i(t) = \exp[-(t - L/c)^2/(2\tau^2)]$ with $\tau = 1 \mu s$, at the output of the medium as a function of the mean photon number of the squeezed vacuum N , for the different values of Ω considered in Fig. 3(a). We have used the analytical approach given by Garrett and McCumber [42], thus we have considered in the computation the dispersion in both the real and imaginary parts of the refractive index. Note that the case with $\Omega = 0.5\gamma$ (dashed line) allows us to obtain the largest negative value in the time delay ΔT . The counterpart is that in the superluminal regime, the peak height of the transmitted pulse is reduced up to $1/2500$ with regard to that of the incident pulse. By considering $\Omega = 1\gamma$ (dashed-dotted line), the interval of variation in the time delay is smaller in width than in the previous case, whereas the peak reduction of the output pulse is not larger than $1/50$ with regard to that of the incident pulse. A further increase of the Rabi frequency to $\Omega = 1.5\gamma$ (solid line) produces less attenuation throughout all the values of N , although the range of time delay achievable is reduced in comparison to the previous cases.

We have obtained a rough estimation of the absorption at $\omega_p = \omega_L$ as a function of the mean photon number by using a symbolic mathematical package. The absorption can be approximated to

$$\text{Re}[A(\omega_p = \omega_L)] \approx \frac{135}{2} \frac{N^3}{[(\Omega/\gamma)^2 + 18N^2]}. \quad (3.5)$$

From Eq. (3.5) we can see that the linear absorption presents the maximum value of $0.32/(\Omega/\gamma)$ for a mean photon number given by $N_m \approx (\Omega/\gamma)/\sqrt{6}$. For values of N lesser or larger than N_m the absorption at the line center decreases. The estimation provided in Eq. (3.5) would allow us to optimize the value of N which permits pulse propagation with moderate attenuation.

In order to estimate the degree of distortion of the transmitted pulse we analyze how the transmitted pulse deviates from the incident Gaussian pulse. To this purpose we have computed the coefficient of asymmetry C_A and kurtosis K of the normalized transmitted pulse $I_T(t) = |E_T(t)|^2/A$, $E_T(t)$ being the transmitted pulse and A is the area under the curve $|E_T(t)|^2$. We remind here that the moment of order k of the distribution $I_T(t)$ can be computed according to

$$\mu_k = \int_{-\infty}^{\infty} (t - \mu_0)^k I_T(t) dt, \quad k = 1, 2, 3, \dots, \quad (3.6)$$

μ_0 being

$$\mu_0 = \int_{-\infty}^{\infty} t I_T(t) dt. \quad (3.7)$$

The asymmetry and kurtosis parameters are defined as

$$C_A = \frac{\mu_3}{\sigma^3},$$

$$K = \frac{\mu_4}{\sigma^4}. \quad (3.8)$$

It is well known that for a Gaussian distribution these coefficients take the values $C_A = 0$ and $K = 3$, so the deviations from these values of the transmitted pulses will inform us about the distortion produced during propagation. In all the cases considered in Fig. 3 the values for C_A are essentially null except for the case with $\Omega = 0.5\gamma$ and in the range of small values of the mean photon number ($N < 0.07$) where a slight deviation from zero has been found numerically. In particular, we obtain values of C_A in the order of -0.025 . Concerning the kurtosis parameter K the values differ from 3 in the second decimal place for the same range of N as C_A . Of particular interest are the deviations found in the case with $N = 0$, thus indicating that the pulse considered here is distorted during its propagation in spite of the fact that the condition for EIT is achieved. Finally, for the other Rabi frequencies considered in Fig. 3 the values for C_A and K are coincidental with those associated to the Gaussian distribution, thus indicating that the transmitted pulses maintain their Gaussian character. We present in Fig. 4 the transmitted pulses for two different values of the mean photon number and taking $\Omega = 1.5\gamma$. The case corresponding to free-space propagation is also shown. The curves have been normalized to their respective maximum values for comparison purposes. In the absence of squeezed vacuum ($N = 0$), the pulse is delayed around $0.3 \mu s$. In the case with $N = 2$, the pulse is advanced around $0.04 \mu s$. According to solid line in Fig. 3(b) the peak reduction at $N = 2$ is around 0.12 of the initial value.

The squeezed vacuum is a phase-dependent reservoir, so in the present case, the optical response of the atomic system depends on the relative phase (Φ) between the squeezed field and the coherent field [see Eq. (2.8)]. Let us analyze the influence of the relative phase between the coherent field and the squeezed field (Φ) in the group velocity of the probe pulse. Figure 5 displays the slope of the refractive index at $\omega_p = \omega_L$ (dotted line) versus the relative phase Φ for a Rabi frequency $\Omega = \gamma$ and with $N = 1.5$. This curve exhibits a transition from negative to positive values, thus allowing us to produce an externally controlled change of pulse propagation from superluminal to subluminal regime. The real part of the refractive index (solid line) and the linear absorption (dashed line) at $\omega_p = \omega_L$ are also displayed in Fig. 5 versus the relative phase Φ . Note that the small values of the absorption and the refractive index allows us to manipulate the group velocity of a weak electromagnetic pulse with reduced attenuation and distortion by adjusting the relative phase Φ . In conse-

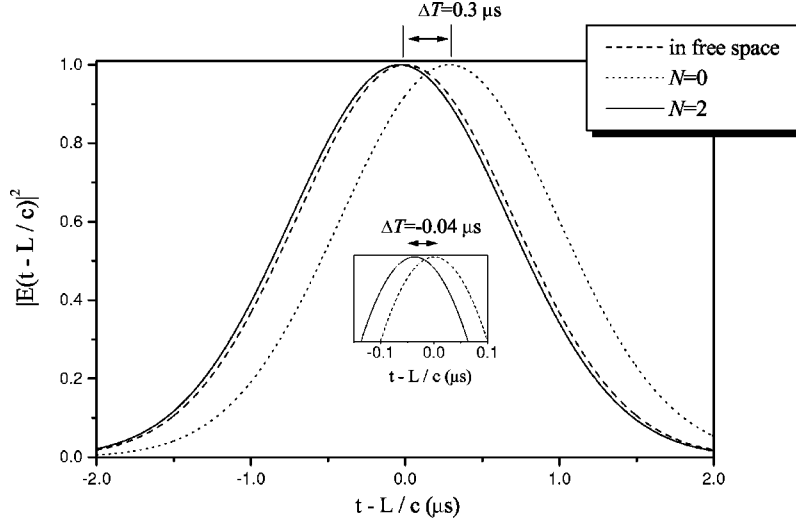


FIG. 4. Pulse propagated through an ultracold medium of atoms with the data of the experiment carried out in Ref. [6]: the solid/dotted line corresponds to superluminal/subluminal propagation ($N=2/N=0$). The dashed line corresponds to free-space propagation. We have used $\Delta_2=0$, $\omega_{21}=0$, $\Omega=1.5\gamma$, $p=0.99$, and $\Phi=0$.

quence, it becomes evident that Φ can be considered as an additional knob for changing pulse propagation from subluminal to superluminal.

IV. DISCUSSION OF THE NUMERICAL RESULTS

In this section we provide a physical interpretation of the spectral features found in the above numerical results. Obtaining non-null absorption at $\omega_p = \omega_L$ when $N \neq 0$, reveals that the EIT condition is broken as a consequence of the interaction of the atom with the squeezed reservoir. This can be understood by considering the population in the field-dependent basis defined as [40]

$$|+\rangle = \frac{\Omega|2\rangle + \Omega_p|1\rangle}{\Omega_T},$$

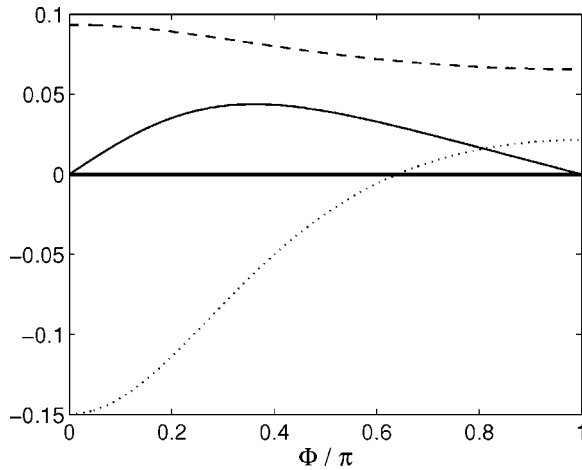


FIG. 5. The slope of the dispersion at $\omega_p = \omega_L$ (dotted line) versus the phase of the squeezed field Φ . The refractive index (solid line) and absorption (dashed line) at $\omega_p = \omega_L$ are also shown. $N=1.5$, $\Omega=\gamma$, $\omega_{21}=0$, and $p=0.99$. The horizontal thick solid line is a reference line that allows to determine the crossing from the subluminal to the superluminal regime.

$$|-\rangle = \frac{\Omega_p|2\rangle - \Omega|1\rangle}{\Omega_T},$$

$$|3\rangle = |3\rangle, \quad (4.1)$$

where $\Omega_T = \sqrt{\Omega^2 + \Omega_p^2}$, Ω_p being the Rabi frequency of the probe field. In this basis we get

$$\rho_{++} = \frac{1}{\Omega_T^2} [\Omega^2 \rho_{22} + \Omega_p^2 \rho_{11} + \Omega_p \Omega (\rho_{21} + \rho_{12})],$$

$$\rho_{--} = \frac{1}{\Omega_T^2} [\Omega_p^2 \rho_{22} + \Omega^2 \rho_{11} - \Omega_p \Omega (\rho_{21} + \rho_{12})], \quad (4.2)$$

here ρ_{++}/ρ_{--} is the population of the bright/dark state. In Fig. 6 we plot ρ_{--} (solid line) and ρ_{++} (dashed line) versus the mean photon number N . It is clearly seen that for $N=0$, $\rho_{--}=1$, i.e., all atoms accumulate in the dark state. While by

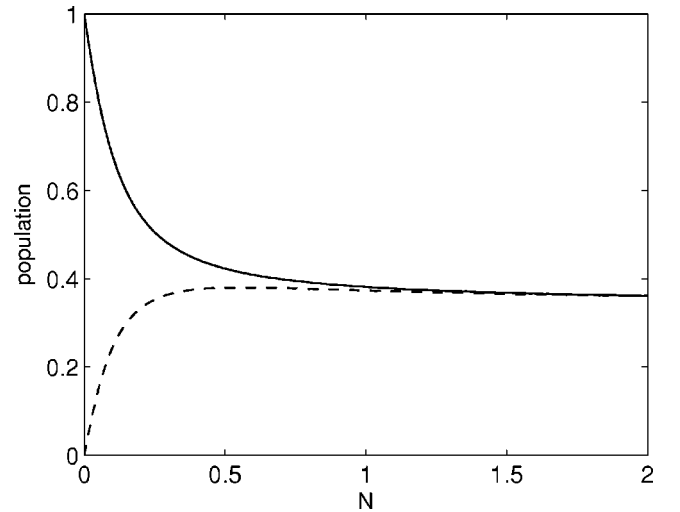


FIG. 6. Population of dark state ρ_{--} (solid line) and bright state ρ_{++} (dashed line) [see Eq. (4.2)] as a function of the mean photon number N . $\Omega=0.5\gamma$, $\omega_{21}=0$, $\Delta_2=0$, $p=0.99$, and $\Phi=0$. The condition $\Omega_p \ll \Omega$ holds.

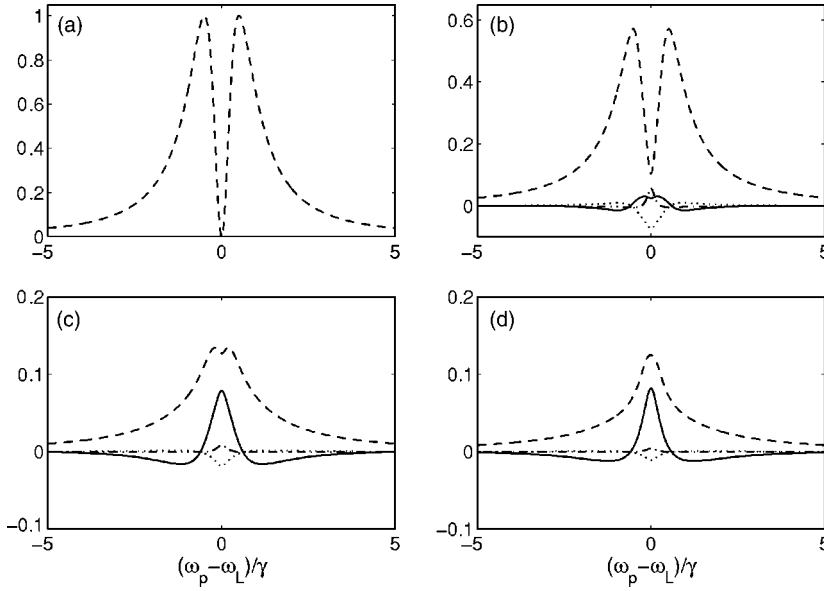


FIG. 7. Different contributions to the real part of the absorption spectrum for the cases considered in Fig. 2. The solid, dashed, dashed-dotted, and dotted curves represent the contribution associated to coherence ρ_{12} , inversion $\rho_{11} - \rho_{33}$, coherence ρ_{13} , and coherence ρ_{23} , respectively [see Eq. (4.3)].

increasing N , the population in the dark state decreases considerably, thus the coherent population trapping effect is destroyed. Moreover, the numerical results demonstrate that the strength of the squeezed vacuum field can alter the behavior of the system in important ways. In particular, by increasing the squeezing photon number N , the EIT condition is broken and it can result in an electromagnetically induced absorption (EIA) at $\omega_p = \omega_L$ [see Fig. 2(c)]. Note that for large values of N the populations of states given in Eq. (4.2) tend to equalize. Since the absorption at $\omega_p = \omega_L$ arises from the transition $|+\rangle \rightarrow |3\rangle$, the increase of N would lead the system to saturation, i.e., a single Lorentzian line shape should be expected instead of the subnatural line numerically found. In order to get a deeper insight into the effect of the SGC and SV on the probe absorption, we separate the absorption spectrum $A(\omega_p)$ obtained in the Appendix as a sum of different contributions. From Eq. (A8) it is easy to show that

$$A(\omega_p) = d_{13}^2 [R_{22}(\bar{\rho}_{11} - \bar{\rho}_{33}) + R_{23}\bar{\rho}_{13} - R_{25}\bar{\rho}_{23} + R_{28}\bar{\rho}_{12}], \quad (4.3)$$

where $\bar{\rho}_{ij}$ are the steady-state values of the elements of the density matrix, and R_{ij} are the (i, j) elements of the matrix R defined in the Appendix. To appreciate how the absorption spectrum is contributed by the different terms, we have plotted in Fig. 7 the individual contributions to $A(\omega_p)$ as a function of the frequency difference $(\omega_p - \omega_L)/\gamma$ when considering the same parameters as in Fig. 2. By comparing Fig. 7 with the spectra displayed in Fig. 2, it becomes evident that as N increases, the contribution of the lower-level coherence term, which is proportional to $\bar{\rho}_{12}$ in Eq. (4.3), becomes more relevant. In fact, there is a competition between the inversion term $(\bar{\rho}_{11} - \bar{\rho}_{33})$ and the lower-level coherence $\bar{\rho}_{12}$ term. For very low values of N , the inversion dominates, showing the EIT-like dip on the absorption. But when N increases, the lower-level coherence term superimposes to the contribution from the inversion term inducing a sharp absorption peak at resonance. Therefore the lower-level coherence term is responsible for the induced absorption appearing in Figs. 2(c)

and 2(d). This anomalous dispersion peak is the physical origin of the superluminal propagation. It should be noted that when setting $M=0$ but $N \neq 0$ (the atom is damped by a thermal field at finite temperature), the sharp absorption peak associated to the lower-level coherence $\bar{\rho}_{12}$ disappear. This is an indication of the importance of two-photon correlation in the obtention of EIA. We would like to note that the appearance of EIA in a four-state N configuration [14–16] is based in the coherence transfer from the excited levels to the lower ones via spontaneous emission. In the usual Λ system, EIA does not occur, but here the combined effect of SV and SGC is the physical origin of EIA. This can be appreciated by looking at the equations of motion (2.8) for ρ_{31} and ρ_{21} . In an ideal Λ system (with $N=0$, $\gamma_{12}=0$), the time evolution of coherence ρ_{31} depends on ρ_{31} and the coherent pumping term ρ_{21} [see Eq. (2.8)]. When the atom is damped by a squeezed reservoir but SGC is not present ($\gamma_{12}=0$), a new term appears associated to the non-null two-photon correlation. The new term, $|M|\gamma_1 e^{-i\Phi}\rho_{13}$, affects the time evolution of coherence ρ_{31} . Thus SV itself introduces a phase-dependent relaxation process in the probe polarization. Thus, in the absence of SGC, the squeezed vacuum modifies the density-matrix equations in an equivalent way as that obtained in a two-level atom. When both SGC and SV are accounted for in the Λ atomic system, two new terms affects the evolution of the probe polarization: the first one is proportional to the mean photon number N while the other involves the two-photon correlation $|M|$. These two new terms, which are pre-multiplied by γ_{12} , produce a spontaneously mediated transfer of the coherence from the driven transition ($|2\rangle \rightarrow |3\rangle$) to the probe transition ($|1\rangle \rightarrow |3\rangle$), which plays a key role in the occurrence of EIA.

We would like to remark that the results obtained in this work differ from other schemes where the control of the group velocity is achieved by an additional field which couples the two atomic sublevels in Λ and V atoms [18–20], or by decay induced interference in Λ and V atoms [19,20]. In these cases, the changes observed in the group velocity are accompanied by amplification or absorption. In our scheme

the control of group velocity is achieved under minor absorption or amplification conditions over a bandwidth in the order of 0.5γ . This point is crucial to experimentally observe the phenomenon, since significant amplification or absorption can overcome the phenomenon due to reshaping of the pulse during the propagation.

V. CONCLUSIONS

In this paper we have investigated the effects of SGC and a SV field in a Λ -type atom with nearly degenerated sublevels, driven by a moderate coherent field. We have analyzed the pump-probe response. We have demonstrated how the application of a squeezed field can change the group velocity of a weak pulse. Specifically, by varying the intensity of SV, the pulse propagation can change from subluminal to superluminal, that is, the intensity of the squeezing field (N) can act as a knob for changing pulse propagation. Besides, for a non-null value of N , the change in the relative phase of the driving field to the squeezed field (Φ) induces a change from one regime to the other in the propagation of a probe pulse. We also demonstrate the possibility of superluminality in a Bose condensate. Furthermore, in our scheme the control of the group velocity is always achieved under nearly transparency conditions over a moderate bandwidth. We have analyzed how the transmitted pulses are attenuated and/or distorted. The numerical simulations show that pulse delays with negligible distortion and controllable attenuation can be achieved by the proper selection of the driving field and the SV parameters. This point makes this configuration very attractive for propagation from slow light to fast light. It is worth mentioning that the superluminal propagation is based on the anomalous dispersion with subnatural linewidth related to EIA, which occurs as a consequence of the spontaneous transfer of coherence from the driven transition to the probe transition. In summary, the model imparts control of the propagation properties of the probe field by changing the mean photon number of the SV reservoir (N) and by varying the relative phase of the driving field to the squeezed field (Φ).

To conclude, we call attention to some conditions required to prove experimentally the theoretical results predicted in this work. One is concerned with the requirement that the squeezed field modes must occupy the whole 4π solid angle of space. This obstacle should be probably avoided by using some sort of cavity system [43] or by using a weak amplitude fluctuating field which mimics the squeezed vacuum [44]. Furthermore, in our calculations we have used squeezing photon numbers N which are now achievable in labora-

tories [45]. It should be noted that quantum interference between the two decay channels may only occur when the transitions involved are nonorthogonal. Several methods to bypass this stringent condition have been proposed [46] and reviewed in an excellent work by Ficek and Swain [47]. It should be remarked that the progress in semiconductor quantum dots and photonic band-gap materials makes it possible to fabricate semiconductors with optical properties similar to that of the atomic systems [48]. So, it could be possible to fabricate a quantum dot with sufficiently close lower levels to allow SGC.

ACKNOWLEDGMENTS

This work was supported by Project Nos. PR3/04-12458 (U.C.M., Spain) and FIS2004-03267 (M.E.C, Spain).

APPENDIX: COMPUTATION OF THE ABSORPTION SPECTRUM

Equation (2.8) can be written in matrix form as

$$\frac{d\vec{B}}{dt} = L_0 \vec{B} + \vec{C}, \quad (\text{A1})$$

L_0 being a 8×8 matrix of coefficients in Eq. (2.8) and \vec{C} a constant vector. The Bloch vector is defined as

$$\vec{B}(t) = [\langle \sigma_{31}(t) \rangle, \langle \sigma_{13}(t) \rangle, \langle \sigma_{33}(t) \rangle, \langle \sigma_{21}(t) \rangle, \quad (\text{A2})$$

$$\langle \sigma_{12}(t) \rangle, \langle \sigma_{22}(t) \rangle, \langle \sigma_{32}(t) \rangle, \langle \sigma_{23}(t) \rangle]^T. \quad (\text{A3})$$

In order to compute the absorption spectrum given in Eq. (3.1) we introduce the deviation of the dipole moment operator from its mean steady-state value as

$$\Delta D^\pm(t') = D^\pm(t') - \langle D^\pm(\infty) \rangle. \quad (\text{A4})$$

Thus the absorption spectrum is given by

$$A(\omega_p) = \int_0^\infty \lim_{t \rightarrow \infty} \{ d_{13}^2 [\langle \Delta \sigma_{13}(\tau) \Delta \sigma_{31}(0) \rangle - \langle \Delta \sigma_{31}(0) \Delta \sigma_{13}(\tau) \rangle] \} e^{-i(\omega_p - \omega_L)\tau} d\tau. \quad (\text{A5})$$

The two-time correlation functions can be obtained by invoking the quantum regression theorem together with the optical Bloch equation (2.8). Thus we define the column vectors

$$U^{3i}(\tau) = [\langle \Delta \sigma_{31}(\tau) \Delta \sigma_{3i}(0) \rangle, \langle \Delta \sigma_{13}(\tau) \Delta \sigma_{3i}(0) \rangle, \langle \Delta \sigma_{33}(\tau) \Delta \sigma_{3i}(0) \rangle, \langle \Delta \sigma_{21}(\tau) \Delta \sigma_{3i}(0) \rangle, \langle \Delta \sigma_{12}(\tau) \Delta \sigma_{3i}(0) \rangle, \langle \Delta \sigma_{22}(\tau) \Delta \sigma_{3i}(0) \rangle, \langle \Delta \sigma_{32}(\tau) \Delta \sigma_{3i}(0) \rangle, \langle \Delta \sigma_{23}(\tau) \Delta \sigma_{3i}(0) \rangle]^T,$$

$$V^{3i}(\tau) = [\langle \Delta\sigma_{3i}(0)\Delta\sigma_{31}(\tau) \rangle, \langle \Delta\sigma_{3i}(0)\Delta\sigma_{13}(\tau) \rangle, \langle \Delta\sigma_{3i}(0)\Delta\sigma_{33}(\tau) \rangle, \langle \Delta\sigma_{3i}(0)\Delta\sigma_{21}(\tau) \rangle, \langle \Delta\sigma_{3i}(0)\Delta\sigma_{12}(\tau) \rangle, \langle \Delta\sigma_{3i}(0)\Delta\sigma_{22}(\tau) \rangle, \langle \Delta\sigma_{3i}(0)\Delta\sigma_{32}(\tau) \rangle, \langle \Delta\sigma_{3i}(0)\Delta\sigma_{23}(\tau) \rangle]^T, \quad i = 1, 2, \quad (\text{A6})$$

where the superindex T stands for transpose.

According to the quantum regression theorem for $\tau > 0$ the vectors $U^{3i}(\tau)$ and $V^{3i}(\tau)$ satisfy

$$\begin{aligned} \frac{d}{dt} U^{3i}(\tau) &= L_0 U^{3i}(\tau), \\ \frac{d}{dt} V^{3i}(\tau) &= L_0 V^{3i}(\tau), \quad i = 1, 2. \end{aligned} \quad (\text{A7})$$

By following the procedure of working in Laplace space we obtain the steady-state absorption spectrum

$$A(\omega_p) = d_{13}^2 \sum_{k=1}^8 R_{2k}(iz) [\Delta U_k^{31}(0) - \Delta V_k^{31}(0)], \quad (\text{A8})$$

where $U_k^{3i}(0)[V_k^{3i}(0)]$ is the steady-state k th component of the vector $U^{3i}(\tau)[V^{3i}(\tau)]$. $R_{jk}(iz)$ is the (j, k) element of the matrix $R(iz)$ defined as

$$R(iz) = (iz\hat{I}_8 - L_0)^{-1},$$

\hat{I}_8 being a 8×8 identity matrix and $z \equiv i(\omega_p - \omega_L)/\gamma_1$.

-
- [1] M. O. Scully, Phys. Rep. **219**, 191 (1992).
 - [2] O. Kocharovskaya, Phys. Rep. **219**, 175 (1992).
 - [3] J. Mompert and R. Corbalán, J. Opt. B: Quantum Semiclassical Opt. **2**, R7 (2000).
 - [4] S. E. Harris, J. E. Field, and A. Imamoglu, Phys. Rev. Lett. **64**, 1107 (1990).
 - [5] S. E. Harris and L. V. Hau Phys. Rev. Lett. **82**, 4611 (1999).
 - [6] L. V. Hau, S. E. Harris, Z. Dutton, and C. H. Behroozi, Nature (London) **397**, 594 (1999); D. Budker, D. F. Kimball, S. M. Rochester, and V. V. Yashchuk, Phys. Rev. Lett. **83**, 1767 (1999).
 - [7] M. D. Lukin, S. F. Yelin, and M. Fleischhauer, Phys. Rev. Lett. **84**, 4232 (2000).
 - [8] M. Fleischhauer and M. D. Lukin, Phys. Rev. A **65**, 022314 (2002).
 - [9] O. Kocharovskaya, Y. Rostovtsev, and M. O. Scully, Phys. Rev. Lett. **86**, 628 (1999).
 - [10] C. P. Sun, Y. Li, and X. F. Liu, Phys. Rev. Lett. **91**, 147903 (2003).
 - [11] R. Y. Chiao, Phys. Rev. A **48**, R34 (1993); A. M. Steinberg and R. Y. Chiao, *ibid.* **49**, 2071 (1994).
 - [12] L. J. Wang, A. Kuzmich, and A. Dogariu, Nature (London) **407**, 277 (2000).
 - [13] A. Lezama, S. Barreiro, and A. M. Akulshin, Phys. Rev. A **59**, 4732 (1999).
 - [14] A. V. Taichenachev, A. M. Tumaikin, and V. I. Yudin, Phys. Rev. A **61**, 011802(R) (1999).
 - [15] C. Goren, A. D. Wilson-Gordon, M. Rosenbluh, and H. Friedmann, Phys. Rev. A **69**, 053818 (2004).
 - [16] A. M. Akulshin, S. Barreiro, and A. Lezama, Phys. Rev. Lett. **83**, 4277 (1999).
 - [17] K. Kim, H. S. Moon, C. Lee, S. K. Kim, and J. B. Kim, Phys. Rev. A **68**, 013810 (2003).
 - [18] G. S. Agarwal, T. N. Dey, and S. Menon, Phys. Rev. A **64**, 053809 (2001).
 - [19] W-H. Xu, J-H. Wu, and J-Y. Gao, Laser Phys. Lett. **1**, 176 (2004).
 - [20] D. Bortman-Arbiv, A. D. Wilson-Gordon, and H. Friedmann, Phys. Rev. A **63**, 043818 (2001).
 - [21] M. S. Bigelow, N. N. Lepeshkin, and R. W. Boyd, Science **301**, 200 (2003).
 - [22] G. S. Agarwal and S. Dasgupta, Phys. Rev. A **70**, 023802 (2004).
 - [23] M. S. Sahrarai, H. Tajalli, K. T. Kapale, and M. S. Zubairy, Phys. Rev. A **70**, 023813 (2004).
 - [24] H. Kang, L. Wen, and Y. Zhu, Phys. Rev. A **68**, 063806 (2003).
 - [25] F. Xiao, H. Guo, L. Li, C. Liu, and X. Chen, Phys. Lett. A **327**, 15 (2004).
 - [26] J. Javanianien, Europhys. Lett. **17**, 407 (1992).
 - [27] X-M. Hu and J.-S. Peng, J. Phys. B **33**, 921 (2000).
 - [28] S. Menon and G. S. Agarwal, Phys. Rev. A **57**, 4014 (1998).
 - [29] J-H. Wu and J-Y. Gao, Phys. Rev. A **65**, 063807 (2002).
 - [30] A. Joshi, W. Yang, and M. Xiao, Phys. Lett. A **315**, 203 (2003).
 - [31] J. Evers, D. Bullock, and C. H. Keitel, Opt. Commun. **209**, 173 (2002).
 - [32] C. W. Gardiner, Phys. Rev. Lett. **56**, 1917 (1986).
 - [33] Z. Ficek, W. S. Smyth, and S. Swain, Opt. Commun. **110**, 555 (1994).
 - [34] M. III Sargent, Phys. Rep., Phys. Lett. **43**, 223 (1978).
 - [35] U. Akram, M. R. B. Wahiddin, and Z. Ficek, Phys. Lett. A **238**, 117 (1998).
 - [36] Z. Ficek and P. D. Drummond, Phys. Rev. A **43**, 6247 (1991); **43**, 6258 (1991).
 - [37] *Quantum Squeezing*, edited by P. D. Drummond and Z. Ficek (Springer-Verlag, Berlin, 2004).
 - [38] G. S. Agarwal, *Quantum Optics*, Springer Tracts in Modern Physics No. 70 (Springer-Verlag, Berlin, 1974).
 - [39] M. O. Scully and M. S. Zubairy, *Quantum Optics* (Cambridge University Press, London, 1997); J-S. Peng and L. Gao-Xiang, *Introduction to Modern Quantum Optics* (World Scientific,

- Singapore, 1998), Chap. 14.
- [40] M. R. Ferguson, Z. Fizek, and B. J. Dalton, *J. Mod. Opt.* **42**, 679 (1995).
- [41] M. R. Ferguson, Z. Fizek, and B. J. Dalton, *Phys. Rev. A* **54**, 2379 (1996).
- [42] C. G. B. Garrett and D. E. McCumber, *Phys. Rev. A* **1**, 305 (1970).
- [43] P. R. Rice and L. M. Pedrotti, *J. Opt. Soc. Am. B* **9**, 2008 (1992).
- [44] P. Zhou and S. Swain, *Phys. Rev. Lett.* **82**, 2500 (1999).
- [45] N. P. Georgiades, E. S. Polzik, K. Edamatsu, H. J. Kimble, and A. S. Parkins, *Phys. Rev. Lett.* **75**, 3426 (1995).
- [46] H. Schmidt and A. Imamoglu, *Opt. Commun.* **131**, 333 (1996).
- [47] Z. Fizek and S. Swain, *J. Mod. Opt.* **49**, 3 (2002).
- [48] O. Kocharovskaya, A. B. Matsko, and Y. Rostovtsev, *Phys. Rev. A* **65**, 013803 (2001).